



Article

Entrapment of Airborne Particles via Simulated Highway Noise-Induced Piezoelectricity in PMMA and EPDM

Mengyao Lyu¹, Som V. Thomas¹, Heng Wei², Julian Wang³, Tiina A. Reponen⁴, Patrick H. Ryan^{4,5,6} and Donglu Shi^{1,*}

- The Materials Science and Engineering Program, Department of Mechanical and Materials Engineering, College of Engineering and Applied Science, University of Cincinnati, Cincinnati, OH 45221, USA; lyumo@mail.uc.edu (M.L.); valicksm@mail.uc.edu (S.V.T.)
- Department of Civil & Transportation Engineering, College of Engineering and Applied Science, University of Cincinnati, Cincinnati, OH 45221, USA; heng.wei@uc.edu
- ³ Architectural Engineering, Penn State University, State College, PA 16801, USA; jqw5965@psu.edu
- Environmental & Public Health Sciences, Medical School, University of Cincinnati, Cincinnati, OH 45221, USA; reponeta@ucmail.uc.edu (T.A.R.); patrick.ryan@cchmc.org (P.H.R.)
- Department of Pediatrics, University of Cincinnati College of Medicine, Cincinnati, OH 45221, USA
- Division of Biostatistics and Epidemiology, Cincinnati Children's Hospital Medical Center, Cincinnati, OH 45229, USA
- * Correspondence: donglu.shi@uc.edu

Abstract: The US highway system features a huge flux of energy transportation in terms of weight, speed, volume, flow density, and noise levels, with accompanying environmental effects. The adverse effects of high-volume traffic cause health concerns for nearby residential areas. Both chronic and acute exposure to PM 2.5 have detrimental effects on respiratory and cardiovascular health, and motor vehicles contribute 25-35% of direct PM 2.5 emissions. In addition to traffic-related pollutants, residing near major roadways is also associated with exposure to increased noise, and both affect the health and quality of life of residents. While regulatory and policy actions may reduce some exposures, engineering means may offer novel and significant methods to address these critical health and environmental issues. The goal of this study was to harvest highway-noise energy to induce surface charge via a piezoelectric material to entrap airborne particles, including PM 2.5. In this study, we experimentally investigated the piezoelectric effect of a polymethyl methacrylate (PMMA) sheet and ethylene propylene diene monomer (EPDM) rubber foam on the entrapment of copper (II)-2,4 pentanedione powder (Cu II powder). Appreciable voltages were induced on the surfaces of the PMMA via mechanical vibrations, leading to the effective entrapment of the Cu II powder. The EPDM rubber foam was found to attract a large amount of Cu II powder under simulated highway noise in a wide range, of 30-70 dB, and at frequencies of 700-1300 Hz, generated by using a loudspeaker. The amount of Cu II powder entrapped on the EPDM rubber-foam surfaces was found to scale with the SPL, but was independent of frequency. The experimental findings from this research provide a valuable base for the design of a robust piezoelectric system that is self-powered by harvesting the wasted sound energy from highway noise and reduces the amount of airborne particles over highways for effective environmental control.

Keywords: piezoelectric; highway noise; particle entrapment; sound energy



Citation: Lyu, M.; Thomas, S.V.; Wei, H.; Wang, J.; Reponen, T.A.; Ryan, P.H.; Shi, D. Entrapment of Airborne Particles via Simulated Highway Noise-Induced Piezoelectricity in PMMA and EPDM. *Energies* **2022**, *15*, 4935. https://doi.org/10.3390/ en15144935

Academic Editors: Francesco Nocera, Roberto Alonso González Lezcano and Rosa Giuseppina Caponetto

Received: 28 May 2022 Accepted: 5 July 2022 Published: 6 July 2022

Publisher's Note: MDPI stays neutral with regard to jurisdictional claims in published maps and institutional affiliations.



Copyright: © 2022 by the authors. Licensee MDPI, Basel, Switzerland. This article is an open access article distributed under the terms and conditions of the Creative Commons Attribution (CC BY) license (https://creativecommons.org/licenses/by/4.0/).

1. Introduction

Road traffic is a major source of airborne PM 2.5 (particles <2.5 μm in size) and noise pollution, both of which are recognized contributors to cardiovascular and other adverse health effects [1]. The association between road-traffic noise and public health has become increasingly evident, especially during the last decade [2]. For instance, the increase in weighted noise level 10 dB(A) within the range of approximately 52–77 dB(A) results in an

Energies **2022**, 15, 4935 2 of 13

8% increase in the risk of cardiovascular diseases [3]. There is a 3% increase in the prevalence of hypertension per 5 dB(A) increase in the noise range of 45–75 dB(A) [3,4]. Additionally, residential traffic noise has the potential to worsen related depressive symptoms [5], mental disorders [6], and insomnia [7]. Furthermore, the PM 2.5 is causally associated with cardiovascular and respiratory health outcomes and co-exposures to both PM 2.5 and noise may have synergistic health effects. Approximately 11.3 million people (or 3.7% of the US population) live within 150 m of major highway infrastructures, placing them at risk for increased exposure to traffic air pollution and associated adverse health outcomes [8]. Time-series analyses suggest that exposure to PM 2.5 has detrimental effects on respiratory health, and motor vehicles contribute from 25% to 35% of direct PM 2.5 emissions [9–16]. Infants or elementary students at schools near heavy transportation infrastructures are particularly susceptible to such air pollutants [17–19].

Exposure to traffic pollution has been associated with adverse health effects, including pulmonary, neurological, and cardiovascular mortality and morbidity [20,21]. Specifically, exposure to traffic-related airborne particles (TRAP) has been associated with the exacerbation of existing asthma and the incidence of asthma among young and adolescent children [18,22,23]. In a previous community-based study in Cincinnati, we observed significant associations between the estimated TRAP exposure and adverse respiratory outcomes in children, including early childhood wheezing, persistent wheezing through age 7, and the development of asthma by age [7,17,24]. The threat from COVID-19 is even more alarming as the severity of COVID-19 infection has been associated with increased PM 2.5 exposure [25–28]. This interaction can occur either directly, by compromising the lungs' immune response to the infection, or indirectly, by exacerbating underlying respiratory or cardiovascular diseases [28].

Sound is typically characterized in terms of two main properties: frequency and intensity. The frequency of sound is the objective measure of its pitch (subjective measure). Cars produce noises in the range of 50 to 5000 Hz, while trucks produce noises in the range of 10 to 1000 Hz. In both cases, the typical noise distribution has a broad intensity peak at about 1250 Hz and a broad perceptual peak at about 500 Hz [29]. Noise barriers are designed to block the sound waves in the propagation path from the source to the receiver. The Environmental Impact Assessment and Noise Impact Assessment determined the types of noise barrier, such as reflective noise barriers, absorptive noise barriers or a combination of both [29]. Improving the acoustic performance of a vertical barrier without increasing its height has long been a challenge to the acoustic engineer. The pure reflective types, even with optimal morphological design and parametric analysis, are still not able to resolve this challenge. Based on a literature review, potential solutions can be classified into three types—absorptive, angled, and capped barriers. The notable developments include vegetation barriers [30,31], parallel noise barriers [16], barriers with absorbent/soft/reactive surfaces [32], diffusive noise barriers [33], T-shaped barriers [34], and other hybrid barrier profiles combined with T-, Y-, and inclined types [35–42].

The dispersion of pollutants from traffic emissions has been shown to be affected by near-road obstacles, such as noise barriers, buildings, and vegetation [43–45]. Depending upon the roadway–barrier configuration, concentration deficits of 50% or more have been observed relative to a reference roadway configuration in the absence of a barrier [17]. Previous studies showed that noise barriers can lead to an upward deflection of airflow caused by the structure. Thus, these barriers could increase the apparent release height of the pollutant, leading to more vertical mixing due to the flow separation at the top of the barrier [46–50]. More importantly, as a huge flux of transport energy in terms of weight, speed, volume, and noise, highway systems generate vast amounts of wasted energy due to inefficient consumption, particularly through large-sized-engine vehicles. The energy from both audible noise and the high flux of heavy-vehicular traffic flows is not only entirely wasted, but also results in traffic-related pollution and adverse health effects.

It is possible to address these critical issues by harvesting highway-noise energy and converting it to electricity via a piezoelectrical material with unique structures. The Energies **2022**, 15, 4935 3 of 13

piezoelectric effect results from the imbalance of the ionic crystal-lattice-based electric dipole moments under mechanical deformation [51,52]. Upon mechanical-pressure-induced deformation, the electric dipole moments are induced for ions on crystal-lattice sites with asymmetric charge surroundings. The noise from highways is a mechanical wave with an oscillation of pressure traveling through a medium. When the sound waves encounter the piezoelectric material with sufficient vibrations, surface charges can be developed on the piezoelectric materials. There are considerable studies on harvesting environmental noise for energy generation. Piezoelectric devices and sensors have been placed within highway structures to harvest noise energy, with significant successes [53]. Field-traffic and sound measurements can be collected in time intervals with the peak hour factor (PHF) to reflect the characteristics of traffic flow. Highway noise is generated from motor vehicles of various sizes and weights, contributing to a spectrum of collective sound energy with an average frequency of road noise of around 1000 Hz [29].

Previous research has mainly concentrated on the areas of noise harvest for energy generation and noise monitoring using piezoelectric materials and devices. No research has been carried out to investigate the possibility of capturing the airborne particles emanating from motor vehicles by using piezoelectric filters. Further, questions remain as to the level of noise that is sufficient to generate enough surface charge for the entrapment of airborne particles of different dimensions, distributions, and weights. In this study, we experimentally investigated the piezoelectric materials of a polymethyl methacrylate (PMMA) sheet and ethylene propylene diene monomer (EPDM) foam for the entrapment of copper (II) 2,4-pentanedionate (Cu II particles) under sound waves of different decibels (dB) and frequencies. Both PMMA and EPDM are known piezoelectric materials with piezoelectric coefficients (d₃₃) of 0.276 pC/N and 1.658 pC/N, respectively. The chosen sound frequencies and decibels are within the range of highway noise levels. Cu II particles are significantly larger and heavier than typical PM 2.5 particles; this allowed us to establish the baseline for the entrapment of most of the airborne particles in terms of size and weight. If a piezoelectric material vibrates in response to highway noise, depending upon the level of vibration, surface charges can be generated that are proportional to the level of noise (in decibels). Most of the airborne particles are surface-charged under various conditions [54–56]. The surface-charged piezoelectric material can therefore electrostatically entrap the airborne particles, including various harmful airborne pollutants, emitted from traffic, such as PM 2.5.

2. Experimental Details

We chose polymethyl methacrylate) (PMMA) for the initial particle entrapment. PMMA is a type of piezoelectric material that can convert mechanical energy to electricity (and vice versa) [57]. PMMA is strong, tough, transparent, lightweight, and inexpensive. The density of PMMA is $1.20~\rm g/cm^3$, which is less than half that of glass, but with much higher impact strength. PMMA is inherently UV-resistant due to its molecular stability. In this study, we used a commercial transparent PMMA sheet with a thickness of $0.15~\rm mm$ as the piezoelectric material to test the surface charge generated at different sound levels and frequencies.

Figure 1 shows the experimental set-up to generate surface charge on PMMA surfaces by a vibration motor (VM). The measurement path is also included in this figure. Commercial DC 3.0V Micro Coin Vibration Motor (VM) was used in this experiment, which can provide a vibration force of 0.6 g @100 g, drawing less than 80 mA. A DC power supply (HEWLETT PACKARD, E3612A, 60 V, 0.5 A or 120 V, 0.25 A) was used to drive the VM at various voltages (1 V, 2 V, 3 V, 4 V, and 5 V), and corresponding vibrations were recorded by an accelerometer (cell-phone software, VibSensor, was used to measure the acceleration). As shown in Figure 1, five PMMA sheets of $2.54 \times 2.54 \text{ cm}^2$ were stacked in parallel and fixed tightly with adhesive tapes at four edges. Before each measurement, the mass of the clean sample (five layers of PMMA sheets) was weighed. The sample was laid horizontally on the VM (Figure 1). The DC power supply was turned on by increasing the

Energies **2022**, 15, 4935 4 of 13

power-supply input voltage to a constant value at 1 V, 2 V, 3 V, 4 V, and 5 V. The voltage generated by piezoelectric material across the two outer PMMA surfaces was measured by closely attaching two parallel copper tape plates on both sides of the sample, as electrodes that were connected to the Keithley 2400.

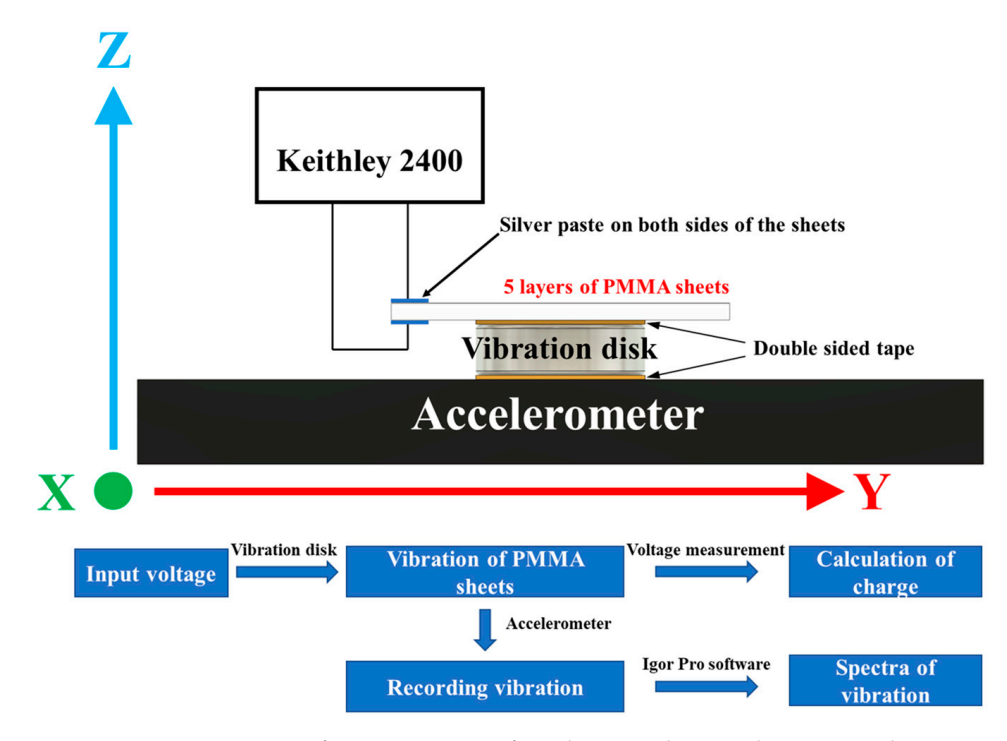


Figure 1. Experiment setup for measuring surface charge and trapped Cu II particles on PMMA.

To simulate the airborne particles, we selected copper (II)-2,4 pentanedionate powder (Cu II powder) for the entrapment experiments. Copper II is used as a catalyst for carbene transfer reactions, coupling reactions, and Michael addition reactions. It is also used as a catalyst for polymerization of olefins and transesterification reactions, as well as a PVC stabilizer. Cu II has a molecular weight of 261.76, which is extremely light, and it is easily absorbed by surface charges created by piezoelectric materials under slight vibrations. The scanning electron microscopy of Cu II particles is shown in Figure 2. As shown in this figure, the Cu II particles exhibit column-like structures, with high aspect ratios. The maximum length of the long axes of the particles was >10 μ m. To capture particles of this size, substantial surface charge needed to be induced by the strong piezoelectric effect of the materials. Experiments based on the Cu II powder ensure effective absorption of airborne PM 2.5 particles, which are much smaller and lighter.

Energies **2022**, 15, 4935 5 of 13

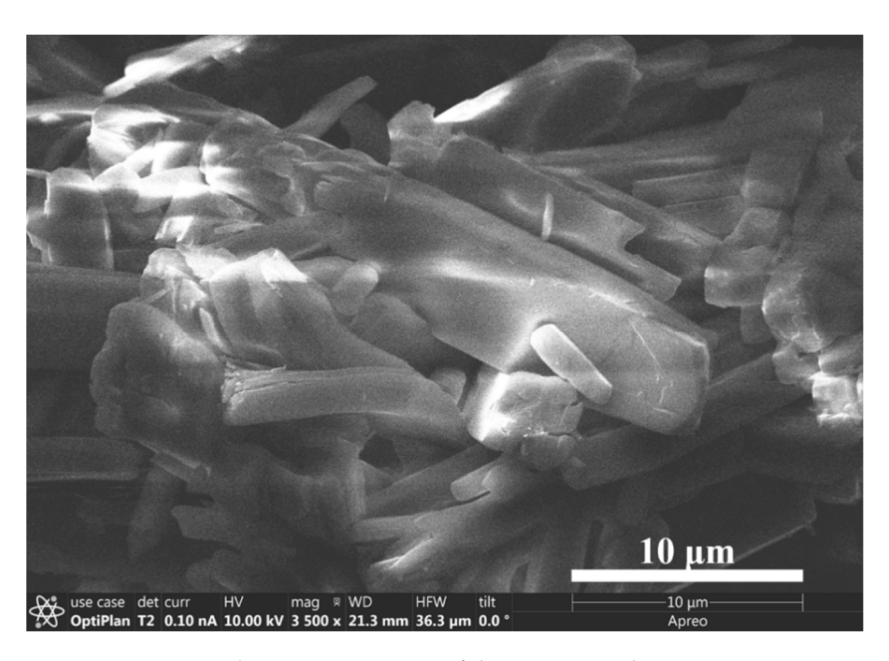


Figure 2. Scanning electron microscopy of the Cu II particles.

3. Results

The PMMA sheets were placed in the set-up, as shown in Figure 1, and the VM was turned on to generate the vibration, whose magnitude was represented by maximum acceleration (m/s²) at a given voltage (1–5 V). Figure 3 shows the maximum acceleration of the vibration generated by the VM at different voltages: 1 V, 2 V, 3 V, 4 V, and 5 V. As shown in Figure 3a,b, the maximum acceleration of the vibration was rather low; it was below 0.1 m/s^2 when the applied voltage of the vibration motor was 1 V (0.037 m/s²) and 2 V (0.051 m/s²). The maximum acceleration of vibration increased to 0.36 m/s^2 at 3 V (Figure 3c), to 0.45 m/s^2 at 4 V (Figure 3d), and to 0.48 m/s^2 at 5 V (Figure 3e), respectively. It should be noted that there was a sharp peak around 14 s at 4 V (Figure 3d), which was disregarded as an anomaly from the background, since it was not sustained enough to affect the particle entrapment.

Figure 4 shows the maximum acceleration vs. the input voltage (Figure 4a), the voltage generated on the PMMA surface vs. the maximum acceleration (Figure 4b), the charge generated on the PMMA surface vs. the maximum acceleration (Figure 4c), and the mass of the trapped Cu II powder on the PMMA surface vs. the voltage. The inset presents a schematic of the Cu II powder attracted on the vertical PMMA surfaces. As shown in Figure 4a, the vibration energy, as indicated by the maximum acceleration, was controlled well by the applied voltage, which could be used to scale with the highway noise level. Due to the piezoelectricity, the vibration induced surface voltage on the PMMA surfaces, as shown in Figure 4b. This figure also shows that the surface voltage induced by the vibration remained quite low, below 10 mV, at the maximum acceleration of the vibration of 0.36 m/s², which appeared to be a threshold value beyond which the induced voltage rapidly increased, up to 981 mV (Figure 4b). The related surface charge as a function of the maximum acceleration of the vibration is shown in Figure 4c. It was calculated based on the surface voltage, Q = CV, where Q is the surface charge, C is the capacitance, and V is the voltage. The capacitance is given by $C = k\epsilon_0 A/d$, where k is the dielectric constant of PMMA, ε_0 is the permittivity of the vacuum, A is the surface area of the PMMA (two outer surfaces), and d is the total thickness of the PMMA. The charge generated by the PMMA sheets was 4.1×10^{-18} C, 9.2×10^{-18} C, 9.2×10^{-17} C, 1.56×10^{-16} C, and 3.36×10^{-16} C for 1 V, 2 V, 3 V, 4 V, and 5 V, respectively, as shown in Figure 4c.

Energies 2022, 15, 4935 6 of 13

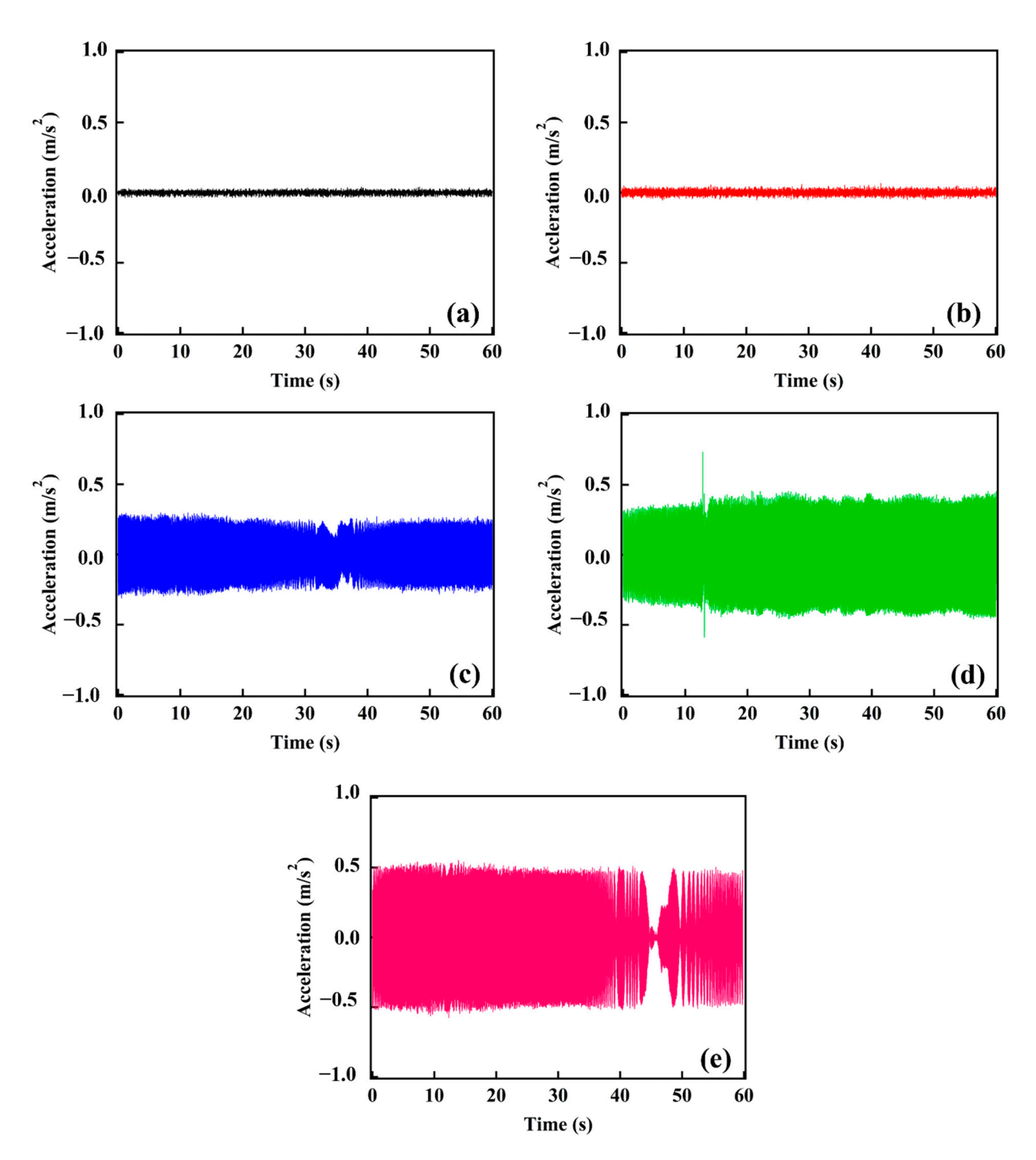


Figure 3. Acceleration of vibration generated by different voltages: (a) 1 V, (b) 2 V, (c) 3 V, (d) 4 V, and (e) 5 V.

The PMMA sheets were placed in the set-up, as shown in Figure 1 and the VM was turned on for 30 s to generate the surface charge at a given voltage (Figure 4b). The VM power supply was then turned off (after 30 s), and the Cu II powder was loosely sprinkled on both surfaces of the PMMA sheets. These PMMA sheets were then positioned vertically to observe the adhered powder on both sides due to the surface charge (inset of Figure 4d). The PMMA sheets with the electrostatically captured powder were weighted using Cole-Parmer Symmetry LA-225.C Analytical Balance to account for the Cu II particles that remained on the two outer surfaces (Figure 4d). As shown in Figure 4d, the mass of the

Energies 2022, 15, 4935 7 of 13

Cu II powder adhered on the PMMA surfaces increased with the input voltage of the VM, reaching 60 mg, at 5 V.

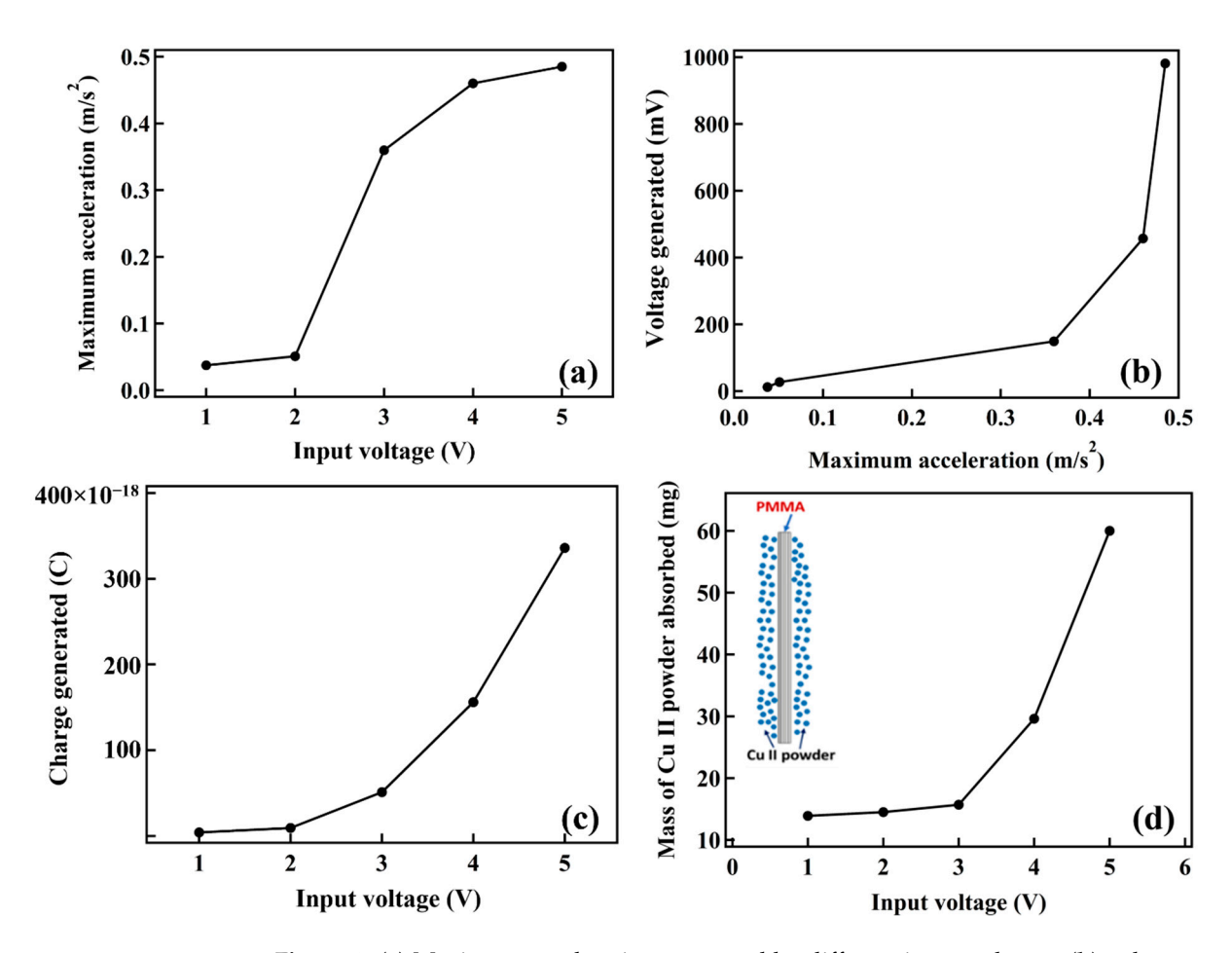


Figure 4. (a) Maximum acceleration generated by different input voltages, (b) voltage generated vs. maximum acceleration of different voltages, (c) charge generated vs. maximum acceleration of different voltages, (d) mass of trapped Cu II powder vs. voltage. Inset: Schematic of Cu II powder adhered on the vertical PMMA surfaces.

Figure 5 shows the photographs of the PMMA sheets with the surface-trapped Cu II powder at different VM input voltages, as indicated. As can be seen in this figure, at low vibration (maximum acceleration), the particles adhered on the surfaces were limited (1–3 V), but at 5 V, a substantial amount of Cu II powder was entrapped on both the outer surfaces of the PMMA sheets, indicating the strong electrical voltages/charges generated by the piezoelectric effect of the PMMA.

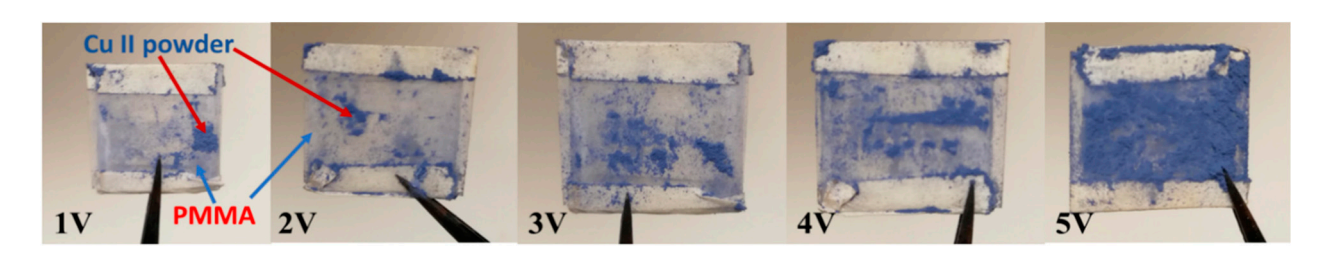


Figure 5. Photographs showing adhered Cu II powder on the PMMA surfaces at different input voltages.

Energies 2022, 15, 4935 8 of 13

Figure 5 shows the significant electric field on the PMMA surfaces generated by a vibrating motor. However, to entrap the airborne particles via traffic noise, the surface charge on the PMMA surfaces had to be generated directly from sound waves with decibels and frequencies comparable to those of a highway. Levels of highway traffic noise typically range from 70 to 80 dB(A) 15 m from highways. Depending upon the size of the vehicles, the highway-noise spectral content is typically dominated by frequencies from 500 to 1000 Hz.

To simulate a more realistic situation for noise-generated surface charge via a piezo-electric material, an experiment was set up for particle capture, as shown in Figure 6, along with the measurement path. A loudspeaker was used to simulate a background noise in a wide range of frequencies and sound pressure levels (SPL). The required frequencies (700–1300 Hz) were generated by a sound-frequency online tone generator. A JBL Cinema 510 5.1 Home Theater Speaker System with a subwoofer (sound source) was connected to a Yamaha 5.1 Channel 4K Ultra HD A/V home-theater receiver. The sound generated was measured and analyzed by cell-phone software called Sound Spectrum Analysis.

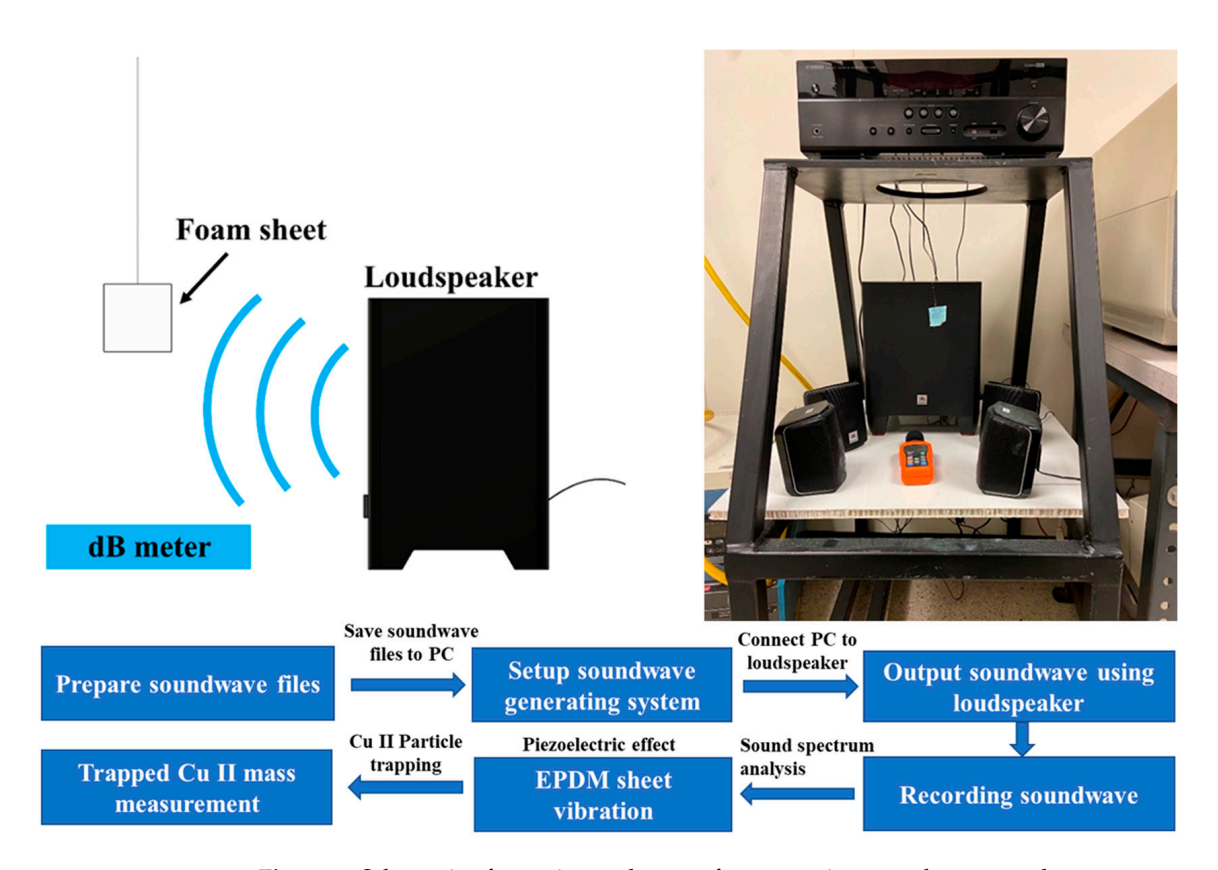


Figure 6. Schematic of experimental set-up for generating sound waves and measurement of particle trapping on EPDM.

For capturing the airborne particles, instead of the PMMA sheets used in the VM vibration experiments, we employed ethylene propylene diene monomer (EPDM) rubberfoam sheets. Ethylene-propylene diene monomer (EPDM) rubber is an excellent soundabsorbing material due to the long-chain structure of the polymer [58]. EPDM also exhibits excellent thermal, mechanical, and electrical properties for a variety of engineering applications [59–62]. EPDM foam has a porous structure that is ideal for the entrapment of airborne particles. Its elastic characteristic enable the efficient absorption of sound waves and conversion to electrical charge on the surfaces.

The EPDM foam sheet was suspended in midair (Figure 6). A Sound Monitor dB Meter (VLIKE LCD Digital Audio Decibel Meter) was positioned adjacent to the EPDM foam sheet that registered the SPL from the sound sources. The distance and the sound

Energies **2022**, 15, 4935 9 of 13

meter between the EPDM foam sheet and the loudspeaker were kept at 25 cm. The speaker was turned on for 30 s at a given SPL and frequency, during which the EPDM foam sheet was vibrated by the sound wave. The speaker was then turned off after 30 s, followed by sprinkling the Cu II powder loosely on both surfaces of the EPDM foam sheet, which was positioned vertically (Figure 6). The EPDM foam sheet with the electrostatically captured Cu II powder was weighed to account for the Cu II particles that remained on the EPDM foam-sheet surfaces (on both sides). The mass of the Cu II particles captured by the EPDM foam sheet was determined under SPL of 30, 40, 50, 60, and 70 dB (referring to sound power intensities of 1, 10, 100, 1000, and 10,000 nW/ m^2 , respectively.) At a given SPL, the mass of the captured powder was also determined at various frequencies (700, 800, 900, 1000, 1100, 1200, and 1300 Hz).

Figure 7a shows the mass of the trapped Cu II particles as a function of the SPL at all frequencies (700–1300 Hz). At 900 and 1000 Hz, the amounts of the trapped Cu II particles were the highest, approaching 800 mg, much higher than those recorded using the vibrating motor (VM), as shown in Figure 4d. It was noted that the highway-noise frequency was around 1000 Hz, which was the optimum range tested in this experiment. Figure 7b shows the masses of the Cu II particles trapped as a function of frequency for different levels of SPL. Quite consistently, in a wide frequency range, between 700 Hz and 1300 Hz, the masses of the trapped Cu II particles were highest at 70dB. These relationships (Figure 7) show the pronounced piezoelectric effect of the EPDM foam sheets, indicating an ideal material candidate for making sound-absorbing and airborne particle-trapping filters for highways. Figure 8 shows the photographs of the EPDM foam sheet with the surface-entrapped Cu II particles (blue color) at different SPL. As shown in this figure, consistent with Figure 7a,b, the amount of Cu II particles increased with increasing SPL, as expected.

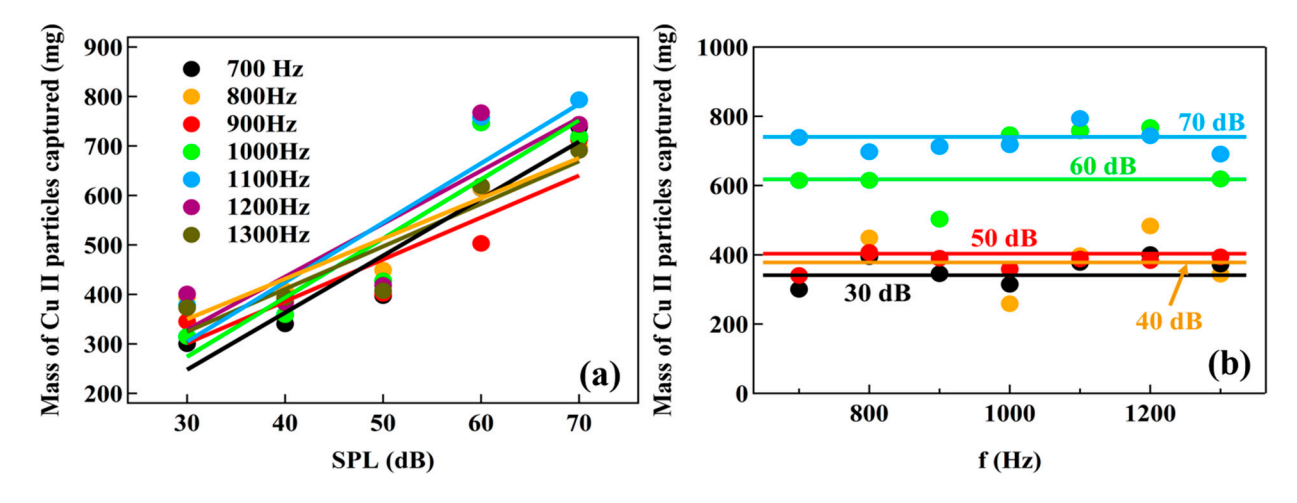


Figure 7. (a) Mass of captured Cu II particle vs. SPL of different frequencies, (b) mass of captured Cu II particle vs. frequency of different SPL.

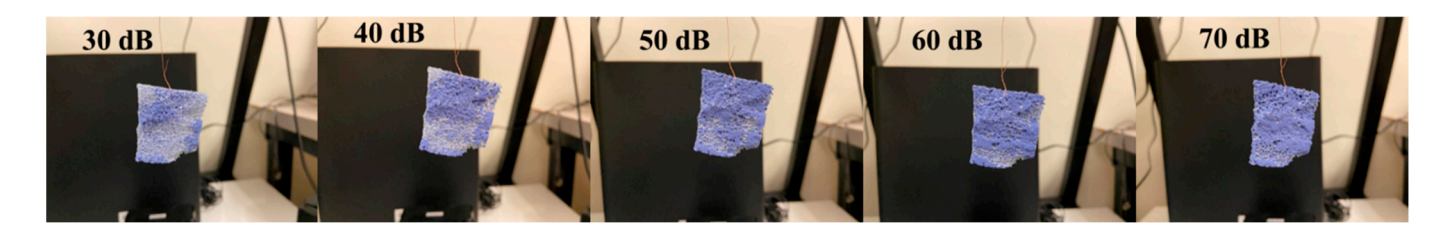


Figure 8. Cu II particles entrapped on the EPDM foam sheet after sound vibration under different SPL (the black box in the background is the loudspeaker).

Energies **2022**, 15, 4935 10 of 13

4. Discussion

There have been extensive studies on airborne-particle captures using various methods. One option to improve the efficiency of mechanical filters is to add electrical charges to the filter material. Examples of these are electret or triboelectric filters. These filters have shown some efficient particle-trapping results, but their efficiency varies with the particle size. Electret filters have been widely used for the filtration of air particles. Since most airborne particles are electrically charged, the capturing mechanism has been typically based on electrostatic interaction. Romay, Liu, and Chae reported o commercially available fibrous electret filters: corona-charged fibrillated split-fiber media, triboelectrically charged mixed-fiber media, and corona-charged melt-blown media [63]. They measured the filtration efficiencies of these filters for different particle sizes and charge states.

Han developed a triboelectric filter for removing PM 2.5 from automobile exhaust fumes using the triboelectrification effect [64,65]. They found that the friction between PTFE (Polytetrafluoroethylene) pellets and electrodes can generate large triboelectric charges and form a space electric field as high as 12 MV/m. By controlling the vibration frequency and fill ratio of the pellets, over 94% of airborne PM 2.5 can be removed using the high electric field in the triboelectric filter. However, the triboelectric filter requires the mounting of the filter in the automobile exhaust system for sufficient mechanical vibrations. The system shown in this study can enable the harvesting of highway noise directly and with much greater sensitivity, making it much simpler, more effective, and more economically viable. In addition, the Cu II power particles are much heavier and larger than the PM 2.5 particles, showing strong electrostatic attraction force on the piezoelectric surfaces.

One of the critical issues in this proof-of-concept study was whether sufficient electrical charge can be generated to create strong enough electrostatic attraction to entrap the Cu II powders and other airborne particles. Although PMMA is a well-known piezoelectric material, the determination of the level of vibration required to generate sufficient surface charge (or voltage) was the first experimental step to be carried out. As shown in Figure 4, even with the small acceleration of vibration, appreciable surface voltages were induced, with a maximum approaching 1000 mV. Within the range of the surface voltage generated, a substantial amount of Cu II particles was captured by the PMMA up to 60 mg, which is quite significant. This correlation between the mechanical vibration/surface charge and the amount of Cu II particles on the PMMA established the baseline and feasibility of airborne entrapment via piezoelectric.

To simulate highway noise, a loudspeaker was employed to generate soundwaves instead of direct mechanical vibration. Sound is typically characterized in terms of two main properties: frequency and sound-pressure levels. For highway traffic, cars produce noise in the range of 50 to 5000 Hz, while trucks produce noise in the range of 10 to 1000 Hz. In both cases, the typical noise distribution has a broad intensity peak at about 1250 Hz and a broad perceptual peak at about 500 Hz [29]. The simulated sound waves used in this study were within the ranges of the highway noise levels (SPL: 30–70 dB, 1 nW/m², frequency: 700–1300 Hz). Successfully, even at the low-noise end of 30 dB in a wide frequency range of 700–1300 Hz, a substantial amount of Cu II powder above 300 mg was captured by the EPDM foam sheet (Figure 7a). The amount of Cu II powder linearly increased with the SPL, up to 800 mg, which is not dependent on frequency (Figure 7b). These experimental results show solid evidence of particle entrapment via sound-generated electrostatic charges using piezoelectric materials. It should be noted that nanoscale piezoelectric materials can be designed and developed with even more airborne particle entrapment.

Another application EPDM foam sheets is to absorb the highway noise in the propagation path from the source to the receiver while harvesting the sound energy for airborne-particle entrapment. EPDM is an excellent soundproofing barrier, especially when it is used on highway edges with high levels of noise. Therefore, EPDM may serve for two purposes: (1) as a sound-insulation barrier to reduce noise pollution, and (2) harvesting noise energy for the entrapment of airborne particles. The Environmental Impact Assessment and Noise Impact Assessment determined different types of noise barrier, such as reflective noise

Energies **2022**, 15, 4935 11 of 13

barriers, absorptive noise barriers, or a combination of both [29]. Improving the acoustic performance of vertical barriers without increasing their height has long been a challenge for acoustic engineers. The pure reflective types, even with optimal morphological designs and parametric analysis, are still not able to resolve this challenge. The system designed in this study could potentially reduce noise levels by engineering the design of acoustic walls with piezoelectric sound absorbers, such as EPDM foam sheets. However, the design of this study is fundamentally different from those of traditional sound barriers, which simply block or reflect highway noise. The EPDM can be utilized to absorb the highway noise and convert the soundwave energy into surface charge via piezoelectricity for the more efficient entrapment of airborne particles of various weights and sizes, including PM 2.5. In this way, the wasted sound energy can be harvested for both noise and airborne-particle reduction.

5. Conclusions

In conclusion, we demonstrated the effective entrapment of Cu II particles by both PMMA and EPDM via the piezoelectric effect. Significant surface charge was generated via mechanical vibrations that enabled the capture of Cu II particles on the PMMA surfaces. The EPDM foam sheets were capable of entrapping Cu II particles effectively in the wide highway-noise ranges of SPL (30–70 dB), sound intensity (1–10 4 nW/m 2), and frequency (700–1300 Hz). The experimental outcomes obtained from this study provide the possibility of reducing highway airborne particles via simple piezoelectric materials. Novel nanoscale structures of piezoelectric materials can also be designed and developed for more efficient airborne-particle entrapment based on the physical principles developed in this study.

Author Contributions: Conceptualization, D.S.; Data curation, M.L. and S.V.T.; Formal analysis, D.S., M.L., S.V.T., H.W., J.W., T.A.R. and P.H.R.; Methodology, D.S., M.L. and S.V.T. All authors have read and agreed to the published version of the manuscript.

Funding: This research was funded by the University of Cincinnati CRA Track 1: PILOTS (Fund Number: D700315).

Institutional Review Board Statement: Not applicable.

Informed Consent Statement: Not applicable.

Data Availability Statement: Data available in a publicly accessible repository.

Conflicts of Interest: The authors declare no conflict of interest.

References

- 1. Meier, R.; Cascio, W.E.; Ghio, A.J.; Wild, P.; Danuser, B.; Riediker, M. Associations of short-term particle and noise exposures with markers of cardiovascular and respiratory health among highway maintenance workers. *Environ. Health Perspect.* **2014**, 122, 726–732. [CrossRef] [PubMed]
- 2. Hammer, M.S.; Swinburn, T.K.; Neitzel, R.L. Environmental noise pollution in the US: Developing an effective public health response. *Environ. Health Perspect.* **2014**, 122, 115–119. [CrossRef] [PubMed]
- 3. Van Kamp, I.; Babisch, W.; Brown, A.L. Environmental noise and health. In *The Praeger Handbook of Environmental Health*; Friis, R.H., Ed.; ABC-CLIO: Santa Barbara, CA, USA, 2012; Volume 1, pp. 69–93, ISBN 978-0-313-38601-5.
- 4. Babisch, W.; Dutilleux, G.; Paviotti, M.; Backman, A.; Gergely, B.; McManus, B. *Good Practice Guide on Noise Exposure and Potential Health Effects*; EEA Technical report; European Environmental Agency: Copenhagen, Denmark, 2010; Volume 11.
- 5. Orban, E.; McDonald, D.; Sutcliffe, R.; Hoffman, B.; Fuks, K.B.; Dragono, N.; Viehmann, A.; Erbel, R.; Jöckel, K.H.; Pundt, N.; et al. Residential road traffic noise and high depressive symptoms after five years of follow-up. *Environ. Health Perspect.* **2016**, 124, 578–585. [CrossRef]
- 6. Sygna, K.; Aasvang, G.M.; Aamodt, G.; Oftedal, B.; Krog, N.H. Road traffic noise, sleep and mental health. *Environ. Res.* **2014**, *131*, 17–24. [CrossRef] [PubMed]
- 7. Evandt, J.; Oftedal, B.; Hjertager Krog, N.; Nafstad, P.; Schwarze, P.E.; Marit Aasvang, G. A population-based study on nighttime road traffic noise and insomnia. *Sleep* **2017**, *40*, zsw055. [CrossRef] [PubMed]
- 8. Meyer, P.; Yoon, P.W.; Kaufmann, R.B. Introduction: CDC Health Disparities and Inequalities Report—United States. *MMWR Supplyments* **2013**, *62*, 3–5.
- 9. Duhme, H.; Weiland, S.K.; Keil, U. Epidemiological analyses of the relationship between environmental pollution and asthma. *Toxicol. Lett.* **1998**, *102*, 307–316. [CrossRef]

Energies **2022**, 15, 4935 12 of 13

10. Hu, S.; McDonald, R.; Martuzevicius, D.; Biswas, P.; Grinshpun, S.A.; Kelley, A.; Reponen, T.; Lockey, J.; LeMasters, G. UNMIX modeling of ambient PM 2.5 near an interstate highway in Cincinnati, OH, USA. *Atmos. Environ.* **2006**, *40*, 378–395. [CrossRef]

- 11. Martuzevicius, D.; Grinshpun, S.A.; Lee, T.; Hu, S.; Biswas, P.; Reponen, T.; LeMasters, G. Traffic-related PM 2.5aerosol in residential houses located near major highways: Indoor versus outdoor concentrations. *Atmos. Environ.* **2008**, 42, 6575–6585. [CrossRef]
- 12. Brunekreef, B.; Holgate, S.T. Air pollution and health. Lancet 2002, 360, 1233–1242. [CrossRef]
- 13. Baldauf, R.W.; Isakov, V.; Deshmukh, P.; Venkatram, A.; Yang, B.; Zhang, K.M. Influence of solid noise barriers on near-road and on-road air quality. *Atmos. Environ.* **2016**, *129*, 265–276. [CrossRef]
- 14. Finn, D.; Clawson, K.L.; Carter, R.G.; Rich, J.D.; Eckman, R.M.; Perry, S.G.; Isakov, V.; Heist, D.K. Tracer studies to characterize the effects of roadside noise barriers on near-road pollutant dispersion under varying atmospheric stability conditions. *Atmos. Environ.* **2010**, *44*, 204–214. [CrossRef]
- 15. NAAQS Table. Available online: https://www.epa.gov/criteria-air-pollutants/naaqs-table (accessed on 16 July 2021).
- 16. United States Environmental Protection Agency. *Transportation Conformity Guidance for Quantitative Hot-Spot Analyses in PM 2.5 and PM10 Nonattainment and Maintenance Areas*; United States Environmental Protection Agency: Washington, DC, USA, 2010.
- 17. Ryan, P.H.; LeMasters, G.K.; Biswas, P.; Levin, L.; Hu, S.; Lindsey, M.; Bernstein, D.I.; Lockey, J.; Villareal, M.; Khurana Hershey, G.K.; et al. A comparison of proximity and land use regression traffic exposure models and wheezing in infants. *Environ. Health Perspect.* 2007, 115, 278–284. [CrossRef] [PubMed]
- 18. Brunekreef, B.; Janssen, N.A.; de Hartog, J.; Harssema, H.; Knape, M.; van Vliet, P. Air pollution from truck traffic and lung function in children living near motorways. *Epidemiology* **1997**, *8*, 298–303. [CrossRef]
- 19. Heinrich, J. Influence of indoor factors in dwellings on the development of childhood asthma. *Int. J. Hyg. Environ. Health.* **2011**, 214, 1–25. [CrossRef]
- 20. Health Effects Institute. Panel on the Health Effects of Traffic-Related Air Pollution. In *Traffic-Related Air Pollution: A Critical Review of the Literature on Emissions, Exposure, and Health Effects*; Special Reort 17; Health Effects Institute: Cambridge, MA, USA, 2010.
- 21. Salvi, A.; Salim, S. Neurobehavioral consequences of traffic-related air pollution. Front. Neurosci. 2019, 13, 1232. [CrossRef]
- 22. Gauderman, W.J.; Avol, E.; Gilliland, F.; Vora, H.; Thomas, D.; Berhane, K.; McConnell, R.; Kuenzli, N.; Lurmann, F.; Rappaport, E.; et al. The Effect of Air Pollution on Lung Development from 10 to 18 Years of Age. *N. Engl. J. Med.* **2004**, *351*, 1057–1067. [CrossRef]
- 23. McConnell, R.; Berhane, K.; Yao, L.; Jerrett, M.; Lurmann, F.; Gilliland, F.; Künzli, N.; Gauderman, J.; Avol, E.D.; Thomas, D.; et al. Traffic, susceptibility, and childhood asthma. *Environ. Health Perspect.* **2006**, *114*, 766–772. [CrossRef]
- 24. Ryan, P.H.; LeMasters, G.K.; Levin, L.; Burkle, J.; Biswas, P.; Hu, S.; Grinshpun, S.; Reponen, T. A land-use regression model for estimating microenvironmental diesel exposure given multiple addresses from birth through childhood. *Sci. Total Environ.* **2008**, 404, 139–147. [CrossRef]
- 25. Wu, X.; Nethery, R.C.; Sabath, M.B.; Braun, D.; Dominici, F. Air pollution and COVID-19 mortality in the United States: Strengths and limitations of an ecological regression analysis. *Sci. Adv.* **2020**, *6*, eabd4049. [CrossRef]
- 26. Tian, T.; Zhang, J.; Hu, L.; Jiang, Y.; Duan, C.; Li, Z.; Wang, X.; Zhang, H. Risk factors associated with mortality of COVID-19 in 3125 counties of the United States. *Infect. Dis. Poverty* **2021**, *10*, 3. [CrossRef] [PubMed]
- 27. Conticini, E.; Frediani, B.; Caro, D. Can atmospheric pollution be considered a co-factor in extremely high level of SARS-CoV-2 lethality in Northern Italy? *Environ. Pollut.* **2020**, *261*, 114465. [CrossRef] [PubMed]
- 28. Travaglio, M.; Yu, Y.; Popovic, R.; Selley, L.; Leal, N.S.; Martins, L.M. Links between air pollution and COVID-19 in England. *Environ. Pollut.* **2021**, 268, 115859. [CrossRef] [PubMed]
- 29. Donavan, P.R.; Janello, C.J. *Mapping Heavy Vehicle Noise Source Heights for Highway Noise Analysis*; No. Project 25-45; Transportation Research Board: Washington, DC, USA, 2017. [CrossRef]
- 30. Van Renterghem, T.; Botteldooren, D.; Verheyen, K. Road traffic noise shielding by vegetation belts of limited depth. *J. Sound Vib.* **2012**, 331, 2404–2425. [CrossRef]
- 31. Lacasta, A.M.; Penaranda, A.; Cantalapiedra, I.R.; Auguet, C.; Bures, S.; Urrestarazu, M. Acoustic evaluation of modular greenery noise barriers. *Urban For. Urban Green.* **2016**, 20, 172–179. [CrossRef]
- 32. Monazzam, M.R.; Fard, S.M.B. Impacts of Different Median Barrier Shapes on a Roadside Environmental Noise Screen. *Environ. Eng. Sci.* **2011**, *28*, 435–441. [CrossRef]
- 33. Cianfrini, C.; Corcione, M.; Fontana, L. Experimental verification of the acoustic performance of diffusive roadside noise barriers. *Appl. Acoust.* **2007**, *68*, 1357–1372. [CrossRef]
- 34. Oldham, D.J.; Egan, C.A. A parametric investigation of the performance of T-profiled highway noise barriers and the identification of a potential predictive approach. *Appl. Acoust.* **2011**, 72, 803–813. [CrossRef]
- 35. Karimi, M.; Younesian, D. Optimized T-Shape and Y-Shape Inclined Sound Barriers for Railway Noise Mitigation. *J. Low Freq. Noise Vib. Act. Control* **2014**, *33*, 357–370. [CrossRef]
- 36. England Health Agent. The Design Manual for Roads and Bridges; England Health Agent: London, UK, 2015.
- 37. Berglund, B.; Hassmén, P.; Job, R. Sources and effects of low-frequency noise. J. Acoust. Soc. Am. 1996, 99, 2985–3002. [CrossRef]
- 38. Twardella, D.; Ndrepepa, A. Relationship between noise annoyance from road traffic noise and cardiovascular diseases: A meta-analysis. *Noise Health* **2011**, *13*, 251. [CrossRef]

Energies **2022**, 15, 4935 13 of 13

- 39. Leventhall, H.G. Low frequency noise and annoyance. Noise Health 2004, 6, 59–72. [PubMed]
- 40. Auerbach, M.; Bockstedte, A.; Zaleski, O.; Von Estorff, O. Numerical and experimental investigations of noise barriers with Helmholtz resonators. In Proceedings of the NOISE-CON 2010, Baltimore, MD, USA, 19–21 April 2010.
- 41. Chintapalli, V.S.N.R.; Padmanabhan, C. An experimental investigation of cavity noise control using mistuned Helmholtz resonators. In *INTER-NOISE and NOISE-CON Congress and Conference Proceedings*; Institute of Noise Control Engineering: Washington, DC, USA, 2014; Volume 249, pp. 1413–1418.
- 42. Yang, C.; Pan, J.; Cheng, L. A mechanism study of sound wave-trapping barriers. J. Acoust. Soc. Am. 2013, 134, 1960–1969. [CrossRef] [PubMed]
- 43. Bowker, G.E.; Baldauf, R.; Isakov, V.; Khlystov, A.; Petersen, W. The effects of roadside structures on the transport and dispersion of ultrafine particles from highways. *Atmos. Environ.* **2007**, *41*, 8128–8139. [CrossRef]
- 44. Hagler, G.S.; Lin, M.Y.; Khlystov, A.; Baldauf, R.W.; Isakov, V.; Faircloth, J.; Jackson, L.E. Field investigation of roadside vegetative and structural barrier impact on near-road ultrafine particle concentrations under a variety of wind conditions. *Sci. Total Environ.* **2012**, *419*, 7–15. [CrossRef]
- 45. Janhäll, S. Review on urban vegetation and particle air pollution—Deposition and dispersion. *Atmos. Environ.* **2015**, *105*, 130–137. [CrossRef]
- 46. Amini, S.; Ahangar, F.E.; Schulte, N.; Venkatram, A. Using models to interpret the impact of roadside barriers on near-road air quality. *Atmos. Environ.* **2016**, *138*, 55–64. [CrossRef]
- 47. Baldauf, R.; Thoma, E.; Khlystov, A.; Isakov, V.; Bowker, G.; Long, T.; Snow, R. Impacts of noise barriers on near-road air quality. *Atmos. Environ.* **2008**, 42, 7502–7507. [CrossRef]
- 48. Heist, D.K.; Perry, S.G.; Brixey, L.A. A wind tunnel study of the effect of roadway configurations on the dispersion of traffic-related pollution. *Atmos. Environ.* **2009**, *43*, 5101–5111. [CrossRef]
- 49. Steffens, J.T.; Heist, D.K.; Perry, S.G.; Zhang, K.M. Modeling the effects of a solid barrier on pollutant dispersion under various atmospheric stability conditions. *Atmos. Environ.* **2013**, *69*, 76–85. [CrossRef]
- 50. Lindman, J.K. Effect of a noise wall on snow accumulation and air quality. Transp. Res. Rec. 1985, 1033, 79–88.
- 51. Manbachi, A.; Cobbold, R.S.C. Development and Application of Piezoelectric Materials for Ultrasound Generation and Detection. *Ultrasound* **2011**, *19*, 187–196. [CrossRef]
- 52. Gautschi, G. Piezoelectric Sensorics: Force, Strain, Pressure, Acceleration and Acoustic Emission Sensors, Materials and Amplifiers; Springer Science & Business Media: Berlin, Germany, 2002; ISBN 978-3-662-04732-3.
- 53. Walubita, L.F.; Sohoulande Djebou, D.C.; Faruk, A.N.; Lee, S.I.; Dessouky, S.; Hu, X. Prospective of Societal and Environmental Benefits of Piezoelectric Technology in Road Energy Harvesting. *Sustainability* **2018**, *10*, 383. [CrossRef]
- 54. Jang, G.G.; Wiechert, A.I.; Ladshaw, A.P.; Spano, T.; McFarlane, J.; Myhre, K.; Yiacoumi, S.; Tsouris, C. Surface charge of environmental and radioactive airborne particle. *Atmos. Chem. Phys. Discuss.* **2021**, 1–14. [CrossRef]
- 55. Kim, Y.H.; Yiacoumi, S.; Tsouris, C. Surface charge accumulation of particles containing radionuclides in open air. *J. Environ. Radioact.* **2015**, *143*, 91–99. [CrossRef]
- 56. Zhang, L.; Gu, Z.; Yu, C.; Zhang, Y.; Cheng, Y. Surface charges on aerosol particles—Accelerating particle growth rate and atmospheric pollution. *Indoor Built Environ.* **2016**, 25, 437–440. [CrossRef]
- 57. Rende, D.; Schadler, L.S.; Ozisik, R. Controlling Foam Morphology of Poly(methyl methacrylate) via Surface Chemistry and Concentration of Silica Nanoparticles and Supercritical Carbon Dioxide Process Parameters. *J. Chem.* **2013**, 2013, 864926. [CrossRef]
- 58. Wang, K.; Yan, X. Performance analysis of ethylene-propylene diene monomer sound-absorbing materials based on image processing recognition. *EURASIP J. Image Video Process.* **2018**, 2018, 128. [CrossRef]
- 59. Athawale, A.A.; Joshi, A.M. Electronic Applications of Ethylene Propylene Diene Monomer Rubber and Its Composites. In *Flexible and Stretchable Electronic Composites*; Ponnamma, D., Sadasivuni, K.K., Wan, C., Thomas, S., AlMa'adeed, M.A.A., Eds.; Springer: Coventry, UK, 2015; pp. 305–333, ISBN 978-3-319-23663-6.
- 60. Bizhani, H.; Katbab, A.A.; Lopez-Hernandez, E.; Miranda, J.M.; Lopez-Manchado, M.A.; Verdejo, R. Preparation and Characterization of Highly Elastic Foams with Enhanced Electromagnetic Wave Absorption Based On Ethylene-Propylene-Diene-Monomer Rubber Filled with Barium Titanate/Multiwall Carbon Nanotube Hybrid. *Polymers* 2020, 12, 2278. [CrossRef]
- 61. Dai, C.; Wu, J.; Zhou, G.; Miao, L.; Yin, Y. Effect of AC Electric Field on Space Charge Distribution in Ethylene Propylene Diene Monomer. In Proceedings of the 2019 IEEE Conference on Electrical Insulation and Dielectric Phenomena, Richland, WA, USA, 20–23 October 2019; pp. 450–453.
- 62. Noh, J.S. Conductive Elastomers for Stretchable Electronics, Sensors and Energy Harvesters. Polymers 2016, 8, 123. [CrossRef]
- 63. Romay, F.J.; Liu, B.Y.; Chae, S.J. Experimental Study of Electrostatic Capture Mechanisms in Commercial Electret Filters. *Aerosol Sci. Technol.* **1998**, 28, 224–234. [CrossRef]
- 64. Han, C.B.; Jiang, T.; Zhang, C.; Li, X.; Zhang, C.; Cao, X.; Wang, Z.L. Removal of Particulate Matter Emissions from a Vehicle Using a Self-Powered Triboelectric Filter. *ACS Nano* **2015**, *9*, 12552–12561. [CrossRef] [PubMed]
- 65. Park, J.H.; Yoon, K.Y.; Noh, K.C.; Byeon, J.H.; Hwang, J. Removal of PM 2.5 entering through the ventilation duct in an automobile using a carbon fiber ionizer-assisted cabin air filter. *J. Aerosol Sci.* **2010**, *41*, 935–943. [CrossRef]